

Unusual thermal expansion of a B–O bond in the structure of danburite $\text{CaB}_2\text{Si}_2\text{O}_8$

Kazumasa Sugiyama and Yoshio Takéuchi

Mineralogical Institute, Faculty of Science, University of Tokyo, Hongo, Tokyo 113,
Japan

Received: October 7, 1985

Danburite / $\text{CaB}_2\text{Si}_2\text{O}_8$ / High-temperature crystal chemistry

Abstract. The crystal structure of danburite has been studied at high temperatures up to 900°C based on single-crystal diffraction intensities collected on a four-circle diffractometer. The thermal response of the structure is basically characterized by an unusual expansion of a specific bond, B–O(2b), of the borate tetrahedron, the thermal expansion coefficient of the bond being $1.6 \times 10^{-5} \text{C}^{-1}$ in the temperature range from about 400°C to 900°C . In accordance with such an expansion, the Ca–O(2b) bond shows a relative contraction with an increase of temperature. The result supports a nine-coordination, rather than seven, for the Ca atom as geometrically defined based on the consideration of Voronoi polyhedron around the atom.

Introduction

The structure of danburite $\text{CaB}_2\text{Si}_2\text{O}_8$ was first analyzed by Dunbar and Machatschki (1931) and later studied by Johansson (1959) and Bakakin, Kravchenko and Belov (1959). The structure is built up of a framework consisting of Si_2O_7 and B_2O_7 groups of tetrahedra; the calcium atom occurs in the eight-membered ring of the framework. A modern refinement of the structure has been made by Phillips, Gibbs and Ribbe (1974). By means of nuclear magnetic resonance spectra of ^{11}B , Brun and Ghose (1964) showed that the B–O–B and Si–O–Si links in the structure persisted up to about 960°C , which is close to the decomposition temperature (Morey and Ingerson, 1937). Danburite is thought to decompose at about 1000°C presumably into cristobalite SiO_2 , B_2O_3 vapour and CaSiO_3 (Brun and Ghose, 1964).

In our high-temperature structural study of various materials having the olivine type [partly published in Takéuchi, Yamanaka, Haga and Hirano (1984)], we noted the following trend of the thermal response of the T–O bonds. Namely, if Pauling's electrostatic valence of the oxygen atom of a T–O bond is oversaturated, the bond shows an anomalous positive expansion. While, if undersaturated, a negative expansion. The structure of danburite is then of particular interest partly because Pauling's electrostatic rule for the oxygen atoms is not obeyed and partly the framework consists of two kinds of tetrahedra having different bulk moduli. We have therefore undertaken a high-temperature structure study of danburite with the result as reported in the present paper.

Experimental

The crystals used for the present study came from Toroku mine, Miyazaki Prefecture, Japan; they were about 30 mm long and had cross section of about 5×5 mm. The chemical composition of danburite from this locality has been reported to be: 48.22 wt% SiO_2 , 0.22 Al_2O_3 , 0.44 Fe_2O_3 , 0.11 MgO , 22.29 CaO , 28.56 B_2O_3 , 0.32 H_2O (Tezuka, 1970). We did not take into account minor components, such as Al, Mg or others, but assumed the ideal chemical composition $\text{CaB}_2\text{Si}_2\text{O}_8$ for structural study which will be described later.

Out of one of the crystals, we prepared an X-ray specimen having the shape of a cylinder, about 15 mm long parallel to c and having a circular cross section with radius 0.15 mm. The cylinder was sealed in a silica-glass capillary and used for X-ray study. With the use of such a crystal specimen, we can evade the possible contamination of the diffraction intensities from the crystal with those from a binder, such as zirconia cement, which is in general used to fix the crystal to a rod.

The crystal specimen was mounted on a goniometer head on a four-circle single-crystal diffractometer AFC5 in such a way that its cylindrical axis was parallel to the ϕ axis. As heat source, we used a miniature electric resistance furnace such as the one described by Brown, Sueno and Prewitt (1973).

The unit-cell dimensions were measured with a single-crystal diffractometer using graphite monochromated $\text{MoK}\alpha$ radiation. The cell dimensions obtained by a least-squares procedure applied to $\sin^2\theta$ values of 20 ~ 25 reflections are listed in Table 1 ($D_x = 2.997 \text{ g cm}^{-3}$, $Z = 4 \times \text{CaB}_2\text{Si}_2\text{O}_8$). The $\omega - 2\theta$ scan technique was used to collect one eighth of the graphite monochromated diffraction intensities up to $2\theta = 60 \sim 110^\circ$. The same cylindrical specimen was used throughout the collection of the sets of diffraction intensities at all temperatures covered. Since we used a collimator having a diameter 0.5 mm to collimate the X-ray beam, the cylindrical crystal specimen was not fully bathed in the X-

Table 1. Variation of cell dimensions with temperature [Å]

| T [°C] | a | b | c | v [Å ³] |
|----------|----------|----------|-----------|-----------------------|
| 25 | 8.037(1) | 8.757(1) | 7.7218(9) | 543.4(1) |
| 104 | 8.041(2) | 8.759(2) | 7.725(1) | 544.1(2) |
| 208 | 8.046(2) | 8.765(2) | 7.734(1) | 545.4(2) |
| 305 | 8.054(2) | 8.768(2) | 7.741(1) | 546.7(2) |
| 407 | 8.061(4) | 8.777(4) | 7.745(2) | 548.0(4) |
| 512 | 8.069(2) | 8.780(2) | 7.757(1) | 549.6(2) |
| 618 | 8.078(2) | 8.786(2) | 7.762(1) | 550.8(2) |
| 720 | 8.083(2) | 8.791(2) | 7.771(1) | 552.3(2) |
| 817 | 8.092(1) | 8.796(1) | 7.7768(8) | 553.6(1) |
| 910 | 8.101(2) | 8.801(2) | 7.786(1) | 555.1(2) |

Table 2. Intensity-study data. The figures in parentheses are the case in which the reflections with $y < 0.65$ were included

| | 25°C | 208°C | 407°C | 618°C | 817°C | 910°C |
|--|--------------------|--------------------|--------------------|--------------------|--------------------|--------------------|
| Absorption coefficient (cm ⁻¹) | 15.49 | 15.43 | 15.36 | 15.28 | 15.21 | 15.17 |
| 2θ maximum (°) | 110 | 70 | 60 | 60 | 60 | 60 |
| No. of reflections observed | 2401 | 1195 | 829 | 817 | 816 | 802 |
| No. of reflections used | 2320 (2348) | 1130 (1155) | 799 (813) | 775 (792) | 780 (787) | 760 (767) |
| $G_{\text{iso.}}$ ($\times 10^{-4}$) | 12.9(3) | 9.9(5) | 6.9(3) | 6.2(3) | 4.8(3) | 2.6(2) |
| R | 0.0256 (0.0259) | 0.0389 (0.0456) | 0.0283 (0.0320) | 0.0340 (0.0434) | 0.0371 (0.0418) | 0.0332 (0.0355) |
| R_w | 0.0322 (0.0326) | 0.0465 (0.0653) | 0.0323 (0.0365) | 0.0406 (0.0676) | 0.0428 (0.0546) | 0.0373 (0.0412) |

ray beam. It then follows that the effective volume (and absorption) of the crystal varies depending upon the orientation of the cylinder with respect to the X-ray beam. Due correction of the observed intensities for the effect was therefore made using the procedure developed by Haga and Takéuchi (1983) after correcting for Lorentz and polarization factors. The intensities thus corrected were finally reduced to structure factors. The intensity fluctuations of three reference reflections, which were measured every 100 reflections at each temperature, was less than $1 \sigma(I)$. Details of the intensity study data are summarized in Table 2.

Refinement

Among structure factors thus obtained, those greater than $3\sigma|F_o|$ were used for structural study (Table 2). The structural data reported by Phillips et al. (1974) served for providing initial coordinates and isotropic temperature factors of the atoms. The refinement of the structure in each case was carried out in space group *Pnam* using the least-squares program LINUS (Coppens and Hamilton, 1970). Unit weight was applied to each reflection.

Anisotropic refinement revealed the existence of conspicuous extinction effects; the correction factor, γ , for the 002 reflection, for example, was as small as 0.31. A correction for the isotropic extinction effect was therefore made using LINUS. The resulting G parameter at each temperature is given in Table 2. It is notable that G is significantly reduced with increasing temperature. The anisotropic refinement at each temperature converged at a value of R as given in Table 2.

A trial was finally made of refining the structure based on a new set of structure factors including only those reflections whose γ 's were greater than 0.65. The resulting atomic coordinates were found to be the same, within the limit of the estimated error, as those obtained from the initial set of structure factors. Even the differences in the values of anisotropic temperature factor coefficients between the two cases did not exceed three times the estimated error. For computations we used neutral atomic form factors for all atoms (*International Tables for X-ray Crystallography*, 1962).

Result and discussion

The final atomic parameters are listed in Table 3 and some important bond lengths and angles in Table 4¹. The structure data at room temperature are essentially the same as those reported by Phillips et al. (1974). Since the thermal behavior of the BO_4 and SiO_4 tetrahedra may best be interpreted considering the Ca–O bonding, we first discuss the geometrical features in the arrangement of oxygen atoms about Ca.

The number of direct oxygen neighbors of Ca

As shown in Figure 1, the oxygen neighbors of the Ca atom are arranged in an irregular fashion. Phillips et al. (1974) favored a sevenfold coordination for the Ca atom based on the mean Ca–O bond length, the O(2b) atom at a distance of 3.017(1) Å (at 25°C) being omitted. The present high-temperature study, however, revealed a significant contribution of Ca to

¹ Listings of anisotropic temperature factor coefficients, individual O–O distances and tetrahedral angles may be obtained referring the no. CSD 51333, names of the authors and citation of the paper at the Fachinformationszentrum Energie-Physik-Mathematik, D-7514 Eggenstein-Leopoldshafen 2, Federal Republic of Germany

Table 3. Fractional atomic coordinates and equivalent isotropic temperature factors (\AA^2)

| | | 25°C | 208°C | 407°C | 618°C | 817°C | 910°C |
|------|-----------------|-------------|-------------|-------------|-------------|-------------|-------------|
| Ca | <i>x</i> | 0.38555(3) | 0.38657(8) | 0.38733(8) | 0.3881(1) | 0.3889(1) | 0.3892(1) |
| | <i>y</i> | 0.07648(3) | 0.07657(7) | 0.07669(7) | 0.0767(1) | 0.0768(1) | 0.0768(1) |
| | <i>z</i> | 0.25 | 0.25 | 0.25 | 0.25 | 0.25 | 0.25 |
| | B_{eq} | 0.514 | 1.066 | 1.336 | 1.726 | 2.127 | 2.328 |
| B | <i>x</i> | 0.2589(1) | 0.2593(3) | 0.2599(3) | 0.2608(3) | 0.2641(4) | 0.2619(3) |
| | <i>y</i> | 0.4192(1) | 0.4190(3) | 0.4190(2) | 0.4189(3) | 0.4191(3) | 0.4186(3) |
| | <i>z</i> | 0.4206(1) | 0.4206(3) | 0.4206(3) | 0.4203(4) | 0.4200(4) | 0.4197(4) |
| | B_{eq} | 0.426 | 0.835 | 0.943 | 1.098 | 1.302 | 1.412 |
| Si | <i>x</i> | 0.05333(3) | 0.05381(7) | 0.05432(6) | 0.05489(8) | 0.05545(9) | 0.05564(8) |
| | <i>y</i> | 0.19250(3) | 0.19252(6) | 0.19252(6) | 0.19258(7) | 0.19272(8) | 0.19260(7) |
| | <i>z</i> | −0.05574(3) | −0.05598(7) | −0.05619(7) | −0.05643(9) | −0.05656(9) | −0.05649(9) |
| | B_{eq} | 0.295 | 0.638 | 0.714 | 0.899 | 1.057 | 1.167 |
| O(1) | <i>x</i> | 0.19291(8) | 0.1930(2) | 0.1935(2) | 0.1938(2) | 0.1942(3) | 0.1944(3) |
| | <i>y</i> | 0.06797(7) | 0.0679(2) | 0.0683(2) | 0.0681(2) | 0.0681(2) | 0.0684(2) |
| | <i>z</i> | −0.00324(9) | −0.0038(2) | −0.0045(2) | −0.0052(3) | −0.0055(3) | −0.0061(3) |
| | B_{eq} | 0.599 | 1.154 | 1.405 | 1.759 | 2.128 | 2.324 |
| O(2) | <i>x</i> | 0.12632(7) | 0.1266(2) | 0.1270(2) | 0.1273(2) | 0.1279(3) | 0.1281(2) |
| | <i>y</i> | 0.36496(6) | 0.3649(2) | 0.3646(1) | 0.3646(2) | 0.3642(2) | 0.3641(2) |
| | <i>z</i> | −0.04233(9) | −0.0417(2) | −0.0413(2) | −0.0412(3) | −0.0410(3) | −0.0404(3) |
| | B_{eq} | 0.498 | 1.012 | 1.159 | 1.483 | 1.802 | 1.920 |
| O(3) | <i>x</i> | 0.39965(7) | 0.4006(2) | 0.4016(2) | 0.4024(2) | 0.4031(3) | 0.4032(2) |
| | <i>y</i> | 0.31351(7) | 0.3138(2) | 0.3143(2) | 0.3145(2) | 0.3150(2) | 0.3151(2) |
| | <i>z</i> | 0.07820(8) | 0.0779(2) | 0.0776(2) | 0.0773(3) | 0.0768(3) | 0.0766(3) |
| | B_{eq} | 0.490 | 0.950 | 1.125 | 1.432 | 1.704 | 1.882 |
| O(4) | <i>x</i> | 0.5137(1) | 0.5125(3) | 0.5117(3) | 0.5116(4) | 0.5108(4) | 0.5102(4) |
| | <i>y</i> | 0.6640(1) | 0.6651(3) | 0.6658(3) | 0.6666(4) | 0.6678(4) | 0.6676(4) |
| | <i>z</i> | 0.25 | 0.25 | 0.25 | 0.25 | 0.25 | 0.25 |
| | B_{eq} | 0.610 | 1.129 | 1.389 | 1.787 | 2.165 | 2.299 |
| O(5) | <i>x</i> | 0.1838(1) | 0.1849(3) | 0.1857(3) | 0.1865(4) | 0.1878(4) | 0.1882(4) |
| | <i>y</i> | 0.4282(1) | 0.4274(3) | 0.4270(3) | 0.4259(4) | 0.4256(4) | 0.4250(4) |
| | <i>z</i> | 0.25 | 0.25 | 0.25 | 0.25 | 0.25 | 0.25 |
| | B_{eq} | 0.590 | 1.116 | 1.341 | 1.747 | 2.054 | 2.205 |

Table 4. Some important bond lengths and bond angles

| | 25°C | 208°C | 407°C | 618°C | 817°C | 910°C |
|------------------------|--------------------|------------|------------|------------|------------|------------|
| Tetrahedron about Si | | | | | | |
| Si—O(1) | 1.618(1) Å | 1.615(2) Å | 1.615(2) Å | 1.616(2) Å | 1.619(2) Å | 1.616(2) Å |
| Si—O(2) | 1.623(1) | 1.624(2) | 1.624(2) | 1.625(2) | 1.623(3) | 1.624(2) |
| Si—O(3) | 1.612(1) | 1.611(3) | 1.610(2) | 1.612(2) | 1.612(2) | 1.613(1) |
| Si—O(4) | 1.613(1) | 1.611(1) | 1.610(1) | 1.612(1) | 1.612(2) | 1.613(1) |
| Mean | 1.616 _o | 1.615(1) | 1.615(1) | 1.616(1) | 1.617(1) | 1.617(1) |
| Mean O—O | 2.638(1) | 2.637(1) | 2.636(1) | 2.639(1) | 2.639(1) | 2.639(1) |
| Vol. (Å ³) | 2.163(1) | 2.159(3) | 2.158(3) | 2.164(3) | 2.164(4) | 2.165(4) |
| Tetrahedron about B | | | | | | |
| B—O(1) | 1.481(1) | 1.481(3) | 1.481(2) | 1.479(3) | 1.478(4) | 1.482(3) |
| B—O(2) | 1.498(1) | 1.498(3) | 1.500(3) | 1.506(3) | 1.511(4) | 1.512(3) |
| B—O(3) | 1.461(1) | 1.465(3) | 1.466(2) | 1.466(3) | 1.468(4) | 1.464(3) |
| B—O(5) | 1.451(1) | 1.450(2) | 1.452(2) | 1.453(3) | 1.451(3) | 1.451(3) |
| Mean | 1.472 ₈ | 1.473(1) | 1.475(1) | 1.476(1) | 1.477(2) | 1.477(2) |
| Mean O—O | 2.403(1) | 2.403(1) | 2.406(1) | 2.408(1) | 2.409(1) | 2.410(1) |
| Vol. (Å ³) | 1.629(1) | 1.631(2) | 1.636(2) | 1.639(3) | 1.642(3) | 1.643(3) |
| Si—O(1)—B | 132.94(6)° | 132.6(2)° | 132.6(2)° | 132.5(2)° | 132.3(2)° | 132.3(2)° |
| Si—O(2)—B | 126.29(4) | 126.5(1) | 126.7(1) | 126.7(2) | 127.0(2) | 127.0(2) |
| Si—O(3)—B | 128.15(5) | 128.4(1) | 128.7(1) | 129.0(2) | 129.4(2) | 129.6(2) |
| Si—O(4)—Si | 136.84(6) | 137.4(2) | 137.6(2) | 137.6(2) | 137.9(3) | 138.1(2) |
| B—O(5)—B | 130.40(6) | 130.9(2) | 131.0(2) | 131.0(2) | 131.3(3) | 131.2(2) |
| Polyhedron about Ca | | | | | | |
| Ca—O(1) × 2 | 2.495(1) | 2.507(2) | 2.516(2) | 2.528(2) | 2.537(3) | 2.543(2) |
| Ca—O(2a) × 2 | 2.452(1) | 2.459(2) | 2.468(2) | 2.473(2) | 2.481(2) | 2.488(2) |
| Ca—O(3) × 2 | 2.466(1) | 2.471(2) | 2.479(1) | 2.485(2) | 2.493(2) | 2.496(2) |
| Ca—O(5) | 2.398(1) | 2.401(1) | 2.405(1) | 2.410(1) | 2.419(1) | 2.422(1) |
| Ca—O(2b) × 2 | 3.017(1) | 3.014(2) | 3.015(2) | 3.018(2) | 3.022(2) | 3.021(2) |
| Mean | 2.584 ₂ | 2.589(1) | 2.596(1) | 2.602(1) | 2.609(1) | 2.613(1) |
| Wt. mean ^a | 2.502 | 2.509 | 2.517 | 2.524 | 2.533 | 2.538 |

^a See text

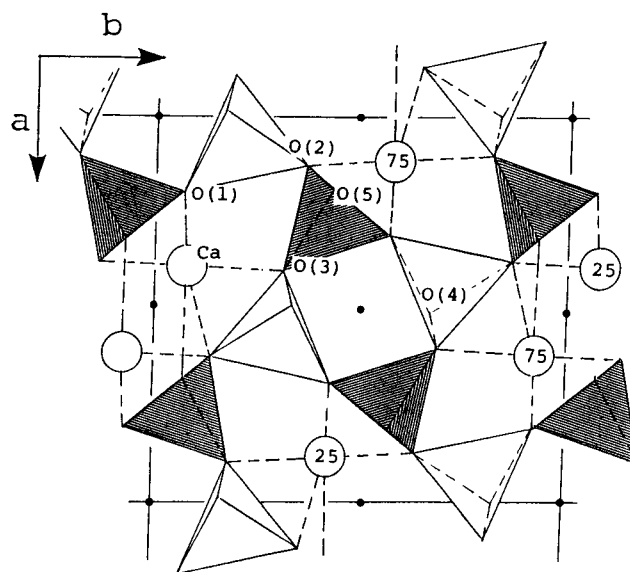


Fig. 1. The structure of danburite viewed down the c axis. Numbers indicate the heights of the Ca atoms in decimal fractions of the c axis. The BO_4 tetrahedra are shadowed. The apices of tetrahedra pointing up are on the mirror plane at $x, y, \frac{3}{4}$ and those pointing down on the mirror plane at $x, y, \frac{1}{4}$.

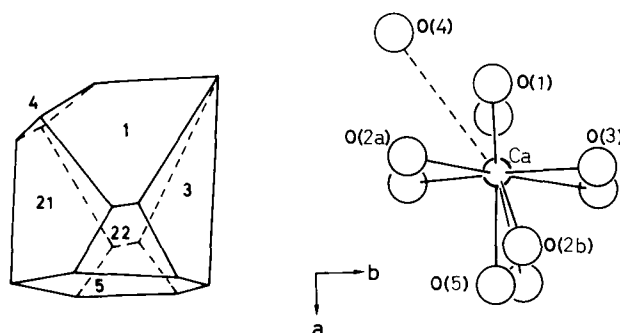
O(2b) (and to its mirror equivalent) as will be shown later. By the aid of Voronoi polyhedra (O'Keeffe, 1979; Takéuchi and Haga, 1984), we then studied the geometrical features characteristic of the arrangement of the oxygen atoms about Ca.

Let $V_c(a)$ denote the Voronoi polyhedron constructed about a cation after excluding the neighboring cations [such a polyhedron has been denoted *O'Keeffe-Voronoi polyhedron* (Takéuchi and Haga (1984))]. Then the ratio $b_i = \theta_i/\theta_o$ may be used to represent the relative contribution of the i th oxygen atom to the surface area of $V_c(a)$, where θ_i is the solid angle subtended by the i th face at the central Ca and θ_o the largest solid angle. The sum of b_i for a total of N faces of $V_c(a)$ corresponds to O'Keeffe's Z^* (O'Keeffe, 1979). In Table 5 we give the area, solid angle and the ratio b_i for each face appearing on $V_c(a)$ constructed about the Ca atom (Fig. 2).

Now, we find that the $V_c(a)$ of the Ca atom has 10 faces, showing that the Ca atom has 10 direct oxygen neighbors (Takéuchi and Haga, 1984). Among those faces, however, the one contributed by O(4) is as small as 0.1, its ratio to Z^* being only about 1.4%. Since that amount of contribution is considered to be negligible, we may conclude that the Ca atom in danburite effectively has 9 direct oxygen neighbors; *i.e.*, the Ca atom is effectively 9-coordinated. This view is consistent with the fact that the maximum bond

Table 5. Characteristics of the O'Keeffe-Voronoi polyhedron constructed about Ca

| Oxygen neighbors | Notation of the face | Area | Solid angle (s. rad.) | b_i | Ca—O distance |
|------------------|----------------------|----------------------|-----------------------|-------|---------------|
| O(1) × 2 | 1 | 4.628 Å ² | 1.612 | 0.881 | 2.496 Å |
| O(2a) × 2 | 21 | 4.186 | 1.644 | 0.898 | 2.452 |
| O(2b) × 2 | 22 | 1.282 | 0.474 | 0.259 | 3.017 |
| O(3) × 2 | 3 | 3.930 | 1.547 | 0.845 | 2.466 |
| O(4) | 4 | 0.140 | 0.183 | 0.100 | 3.656 |
| O(5) | 5 | 4.593 | 1.830 | 1 | 2.398 |

**Fig. 2.** The O'Keeffe-Voronoi polyhedron constructed about Ca (see Table 5), viewed down c but rotated by 5° about b

length for Ca—O has been found to be 3.4 Å based on the procedure provided by Donnay and Allmann (1970). We may now calculate Pauling's valence sum for each oxygen atom, the result showing that O(2b) is oversaturated by 7/36 and O(5) is deficient by 10/36; the remaining O's are much closer to neutral.

In general, each $M-O_i$ bond length of a polyhedron about cation M may be weighted by b_i to calculate the mean $M-O$ bond length for the polyhedron (Takéuchi, 1984). In the present case, the mean Ca—O bond length thus calculated has a value of 2.519 Å at room temperature (Table 5). The weighted mean Ca—O bond lengths listed in Table 4 are those which were calculated based on $V_c(a)$ constructed about Ca by omitting O(4).

Thermal response of the Ca—O bonds

With an increase of temperature, the contribution of O(4) to the surface of $V_c(a)$ decreases only slightly ($b_4 = 0.091$ at 900°C), while that of O(2b)

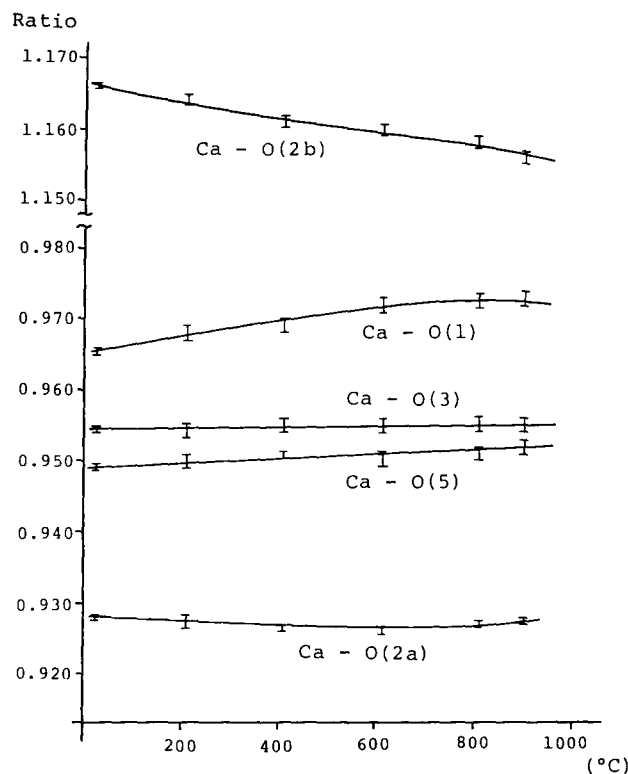


Fig. 3. A plot of the ratio of each individual Ca–O bond length to mean Ca–O versus temperature

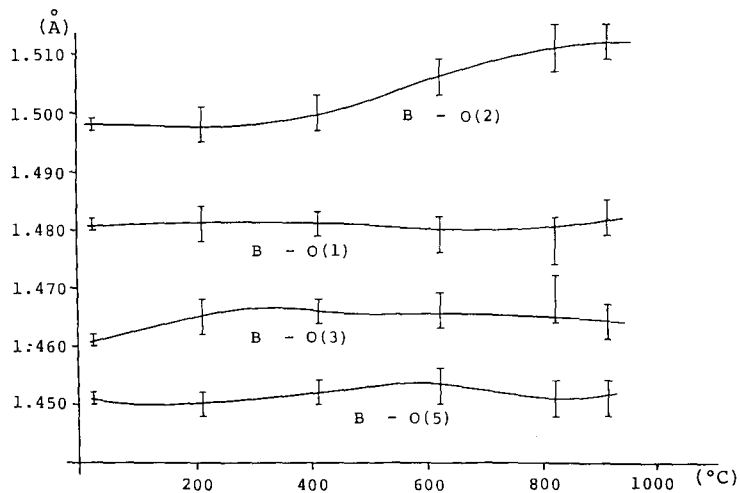


Fig. 4. A plot of individual B–O bond length versus temperature

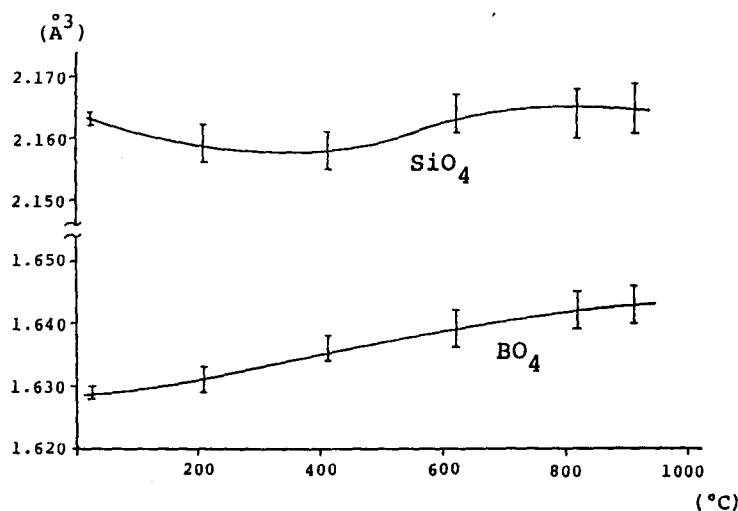


Fig. 5. A plot of the tetrahedral volumes versus temperature

increases significantly, giving $b_{22} = 0.274$ at 900°C . Then if the ratio of each individual Ca–O bond length to the mean Ca–O bond length is plotted versus temperature (Fig. 3), the ratio for Ca–O(2b), the longest Ca–O, shows not an increase but a marked decrease with an increase of temperature. This situation would mean that the bond strength of Ca–O(2b) relatively increases with a raise of temperature. The Ca–O(2b) bond in fact shows the smallest expansion coefficient $0.45 \times 10^{-5}\text{C}^{-1}$. With the exception of this bond, those of the remaining Ca–O bonds are in the range from $5.4 \times 10^{-5}\text{C}^{-1}$ to $2.7 \times 10^{-5}\text{C}^{-1}$ approximately in the decreasing order of the bond lengths (Table 4).

Thermal response of the BO₄ and SiO₄ tetrahedra

In Figure 4, which gives a plot of the B–O bond lengths versus temperature, we observe that B–O(2) shows a marked expansion. Such an expansion may well be accounted for by the above-mentioned relative increase in bond strength of the Ca–O(2) bond with an increase of temperature (Fig. 3). This situation corresponds to the case of the B–O(2) bond in the structure of sinhalite AlMgBO_4 (Takéuchi et al., 1984) having the olivine type structure.

The volume of the BO₄ tetrahedron shows a relatively large rate of expansion between 200°C and 600°C (Fig. 5). Nearly in this temperature range the volume of the SiO₄ tetrahedron shows a slight negative expansion (Fig. 5). Such a change of SiO₄ seems to be related to the relatively significant increase in the Si–O(3)–B and Si–O(4)–Si bond angles (Table 4)

which would be induced by the expansion of BO_4 . Although the individual Si—O bonds as a whole do not show a significant change, the very slight decreasing of Si—O(3) and Si—O(4) at around $200^\circ \sim 400^\circ\text{C}$ (Table 4) is consistent with the above change in the bond angles. While the variance of the tetrahedral angles of SiO_4 is almost invariable throughout the temperature range covered, that of BO_4 increases from $18.1(2)^\circ$ at room temperature to $19.6(8)^\circ$ at 910°C . The thermal response of the danburite structure is thus largely characterized by that of the BO_4 tetrahedra.

Finally, we noted that if the 9-coordinated model is adopted for Ca, the correlation coefficients between T—O bond lengths and parameters, such as $\Sigma 1/(\text{Ca—O})$ or $\Sigma 1/(\text{Ca—O})^2$ (Phillips et al., 1973), are found to be significantly larger compared to those of the case in which a 7-coordinated model is assumed. Namely, for B—O the coefficients are 0.78 (0.54) or 0.74 (0.55), respectively, and for Si—O 0.78 (0.41) or 0.75 (0.41), where the values for the 7-coordinated model are given in parentheses.

Acknowledgement. We thank Dr. N. Haga for his experimental assistance. Computations were carried out on HITAC M-280H at the Computer Center of the University of Tokyo.

References

- Bakakin, V. V., Kravchenko, V. B., Belov, N. V.: The crystalline structure of danburite $\text{CaB}_2\text{Si}_2\text{O}_8$ and hurlbutite $\text{CaBe}_2\text{P}_2\text{O}_8$. Dokl. Akad. Nauk SSSR **129**, 1155–1158 (1959)
- Brown, G. E., Sueno, S., Prewitt, C. T.: A new single-crystal heater for the precession camera and four-circle diffractometer. Am. Mineral. **58**, 698–704 (1973)
- Brun, E., Ghose, S.: Nuclear magnetic resonance spectrum of ^{11}B and B—Si order in danburite, $\text{CaB}_2\text{Si}_2\text{O}_8$. J. Chem. Phys. **40**, 3031–3033 (1964)
- Coppens, P., Hamilton, W. C.: Anisotropic extinction corrections in the Zachariasen approximation. Acta Crystallogr. **A26**, 71–83 (1970)
- Donnay, G., Allmann, R.: How to recognize O^{2-} , OH^{-1} and H_2O in crystal structures obtained by X-rays. Am. Mineral. **55**, 1003–1015 (1970)
- Dunbar, C., Machatschki, F.: Structure of danburite, $\text{CaB}_2\text{Si}_2\text{O}_8$. Z. Kristallogr. **76**, 133–146 (1931)
- Haga, N., Takéuchi, Y.: Absorption and volume corrections for a fine cylindrical sample longer than the beam diameter. In: *Structural Studies of Minerals at High Temperatures and High Pressures*. (Ed. Takéuchi, Y.). J. Miner. Soc. Japan **16**, Spec. Issue **1**, 93–98 (1983)
- International Tables for X-ray Crystallography*. Vol. III. Kynoch Press, Birmingham 1962
- Johansson, G.: A refinement of the crystal structure of danburite. Acta Crystallogr. **12**, 522–525 (1959)
- Morey, G. W., Ingerson, E.: The melting of danburite: A study of liquid immiscibility in the system $\text{CaO—B}_2\text{O}_3\text{—SiO}_2$. Am. Mineral. **22**, 37–47 (1937)
- O'Keefe, M.: A proposed rigorous definition of coordination number. Acta Crystallogr. **A35**, 772–775 (1979)
- Phillips, M. W., Ribbe, P. H., Gibbs, G. V.: Tetrahedral bond length variations in anorthite. Am. Mineral. **58**, 495–499 (1973)
- Phillips, M. W., Ribbe, P. H., Gibbs, G. V.: The crystal structure of danburite: A comparison with anorthite, albite and reedmergerite. Am. Mineral. **59**, 79–85 (1974)

- Takéuchi, Y., Yamanaka, T., Haga, N., Hirano, M.: High-temperature crystallography of olivines and spinels. In: *Materials Science of the Earth's Interior*. (Ed. Sunagawa, I.), pp. 189–229, Terrapub, Tokyo (1984)
- Takéuchi, Y., Haga, N.: Characterization of coordination polyhedra. *Mineral. J.* **12**, 83–86 (1984)
- Takéuchi, Y.: Sphere-packing model of atomic arrangements and coordination polyhedra in inorganic structures. Paul Niggli Symposium, Col. Abst. pp. 59–62, Swiss Soc. Cryst. (1984)
- Tezuka, R.: In: *Introduction to Japanese Minerals* (Ed. Nanbu, M.), p. 198. Geol. Survey of Japan (1970)